AC Loss, Inter-Strand Resistance, and Mechanical Properties of an Option-II ITER CICC up to 30,000 Cycles in the Press

Y. Miyoshi, Y. Ilyin, W. Abbas, and A. Nijhuis

***Abstract*—In Nb_3Sn cable-in-conduit conductors for ITER, the superconducting strands follow complex trajectories defined by the twist pitches of multi-stage cabling and the void fraction of the conductor. The conductor in operation suffers a Lorentz load which results in distributed strand deformations that alter the overall electromagnetic and mechanical behavior of the conductor. With the Twente cable press, a cable specimen is subjected to transverse load up to 30,000 cycles and the changes in the inter-strand contact resistances, the cable deformation, and the coupling loss are monitored. An ITER toroidal field coil conductor with option-II cabling scheme is tested for the first time in the press. In comparison with previously measured conductors, the long twist pitches of option-II result in a higher inter-strand contact resistance, a lower stiffness of the conductor, and initially a higher coupling loss time constant. Within 100 cycles, the time constant decays to a comparable level as the low void fraction conductor with short twist pitches.**

***Index Terms*—CICC, contact resistance, coupling loss, transverse load.**

TABLE I
SAMPLE SPECIFICATIONS

	TFMC-A	TFMC-B	CS1	**EUTF3-EAS**
SC strands	720	720	1152	900
Cu strands	360	360	0	522
Cable layout	$3\times3\times5\times4\times6$	$3\times3\times5\times4\times6$	$3\times4\times4\times4\times6$	$(3\times3\times5\times5$ + core) $\times 6$ core = 3×4 Cu
Twist pitches [mm]	43/ 77-85/ 142/ 160-234/ 416	43/ 77-85/ 142/ 160-234/ 416	45/ 74/ 123/ 160/ 380	80/ 140/ 190/ 300/ 420
Sub-cable covered surface	90 %	90 %	90 %	50 %
Void fraction	26.4 %	29.7 %	36 %	28 %

I. INTRODUCTION

THE Twente cryogenic cable press has been used as a test facility for various types of NbTi and Nb_3Sn cable-in-conduit conductors (CICC) [1]–[6]. The inter-strand contact resistance (R_c) between superconducting strands, the AC magnetization loss and the cable deformation are monitored as a function of load cycles expected from the operating condition of the magnets. Earlier, attempts have been made with an empirical approach, to scale the coupling loss time constant $n\tau$ with the interstrand contact resistance R_c [4] for cables with similar cabling patterns, and to characterize the cable mechanical deformation with loading [6]. Currently, the development of a numerical model of a full size cable to calculate coupling loss is ongoing and its progress is presented in [7]. For the design of practical superconductors in applications, various experimental and theoretical works are performed to investigate the coupling loss of a multistage conductor, and its relationship with the twist pitches and the R_c [8]–[11]. The conductor design is a compromise between its AC and DC transport performance. For example, the design of the ITER toroidal field (TF) coil conductor has been altered to the "option-II" cabling scheme, owing to both predicted [12] and measured [13] improvement in conductors with long twist pitches and low void fraction. We present here the measurement results from the EUTF3-EAS (hereafter EUTF3) conductor, the first of a series of ITER TF conductors with an option-II cabling scheme to be measured by the press up to 30,000 load cycles. The results are compared against prototype Nb_3Sn conductors measured previously. We find a relatively high initial triplet R_c which is interpreted in terms of the first stage twist pitch and the relative ease in the intra-triplet movement. From the cable deformation, we find a correlation between the stiffness of the conductor and the triplet R_c, which indicates the dependence of cable stiffness on overall strand contact area. Finally, we compare the initial values of $n\tau$ to their corresponding initial intra-triplet R_c. We find for this conductor, an initially high $n\tau \sim 680$ ms that decreases with load cycles until a final value ~200 ms.

Manuscript received August 03, 2010; accepted October 12, 2010. Date of publication November 01, 2010; date of current version May 27, 2011. This work was supported in part by the ITER International Organization under Contract 09/4300000059.

Y. Miyoshi, W. Abbas, and A. Nijhuis are with the Low Temperature Division, Faculty of Science and Technology, University of Twente, 7500AE Enschede, The Netherlands (e-mail: y.miyoshi@tnw.utwente.nl).

Y. Ilyin is with the Magnet Division, Building 507/3, TKM, ITER Organisation, 13115 St Paul-lez-Durance, France.

Color versions of one or more of the figures in this paper are available online at http://ieeexplore.ieee.org.

Digital Object Identifier 10.1109/TASC.2010.2088355

II. CONDUCTOR SAMPLE

The conductor features of interest are compared against previously measured conductors in Table I [6]. The longer twist pitches, a low void fraction, and only 50% of the sub- cable surface being covered by the wraps are the characteristic aspects of the option-II cable. The sample with a length of 40 cm

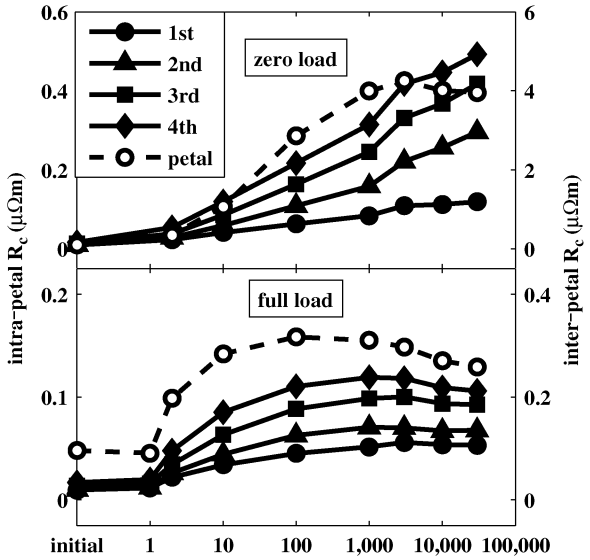

Fig. 1. Evolutions of R_c with cycles at zero load (top) and full load (bottom).

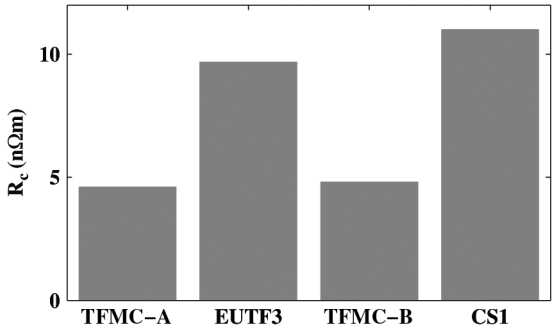

Fig. 2. Initial state intra-triplet contact resistances.

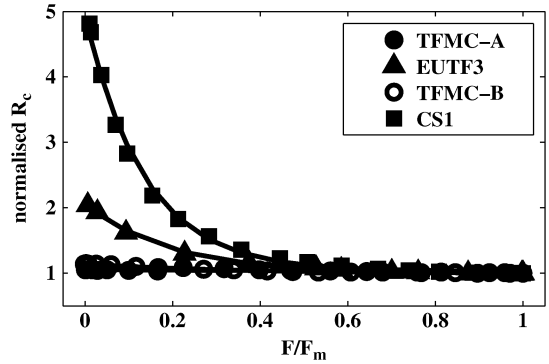

Fig. 3. Normalized intra-triplet R_c while unloading from the maximum applied load F_m at 10,000 cycle. Lines are exponential fits.

is prepared for the press, employing the locked void fraction method. The detailed description of the method is presented elsewhere [4].

The R_c is measured by the four-point method between a pair of individual superconducting strands from different cabling stages. In the previous measurements the inter-petal (final stages) and the inter-bundle (penultimate stages) R_c were measured by strands in the petals and in the bundles, which were soldered together at the current terminals. The cable displacement is measured by six sets of extensometers mounted on the conductor. The AC loss is evaluated from a magnetization loop measured by compensated pick-up coils. The magnetically measured loss is then calibrated by a calorimetric measurement of the loss measured in the virgin condition carried out separately. The applied sinusoidal field has an amplitude 150 mT with a bias level of 350 mT, at frequencies between 10 mHz and 160 mHz.

The sequence for the conductor measurement in the press is as follows. The R_c and the AC loss from magnetization are measured first in the initial condition in the press at 4.2 K, without any applied load. Then, the transverse load is applied in steps up to a designated maximum load for the conductor (580 kN/m for EUTF3). At each loading step, the cable displacement is measured as well as the intra-triplet R_c. At fully loaded state, the R_c and the AC loss measurements are repeated. This is then followed by stepwise unloading, together with the displacement and the triplet R_c measurements. The press automatically undergoes load cycles and at each of the selected cycle, the same measurement procedure is repeated.

III. R_C, Void Fraction and Twist Pitches

The change in R_c with cycles (Fig. 1) shows an initial increase in resistance followed by saturation beyond 1,000 cycles at full load, while no saturation is observed at zero load.

Initially low R_c increase with load cycles as the strands disengage from their initial state after the heat treatment. The saturation with cycles under full load is interpreted as a signature of initially large plastic deformation of the cable that eventually saturates with cycles. We do not observe any abrupt changes in the R_c that may be caused by strand breakages such as crack propagation. This behavior is similar to what has been observed in the prototypes. The initial intra-triplet (1st stage) R_c is $\sim 10\ \mathrm{n\Omega m}$ (Fig. 2) and the initial inter-petal (5th stage) R_c is $\sim 100\ \mathrm{n\Omega m}$. In comparison with the prototypes of similar void fraction, the triplet R_c is relatively high. The inter-petal R_c is approximately two orders of magnitude smaller due to the reduced surface coverage by the sub-cable wraps.

We interpret the relatively high triplet R_c by considering the overall contact area between the strands. The overall contact area can be regarded as a function of the number of crossing points and the area of line contacts, similarly to the numerical models of a multistage conductor [10], [11].

Previous measurements show that the triplet R_c differs clearly between low void fraction (TFMCs) and high void fraction (CS1) conductors and that the change in resistance becomes smaller as the number of cycles increases [5]. The influence of void fraction on the triplet R_c is observed by the evolution of R_c upon unloading from the fully loaded state. We show here the data from the 10,000th cycle since we may assume most strands have become disengaged from their initial state at a high number of cycles. When the cable is unloaded, it expands until it becomes limited by the bolts that secure the initial void fraction of the conductor. Hence, the resistance-load profile reflects the triplet R_c dependence on the free space available for expansion. The R_c dependence on load can be fitted by an exponential function [14] and the R_c normalized to the full load value is shown in Fig. 3. For the TFMCs, the change in R_c by unloading is only $\sim$10%, while EUTF3,

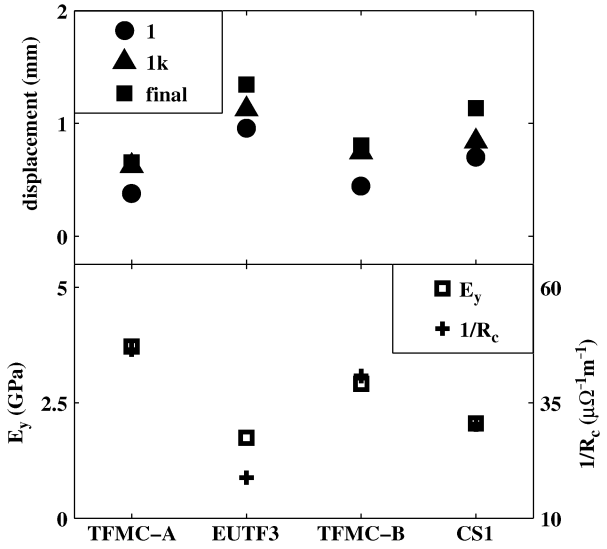

Fig. 4. Top: Cable compressions at maximum load at selected cycles. Bottom: E_y and $1/R_c$ measured at the final cycle at maximum load.

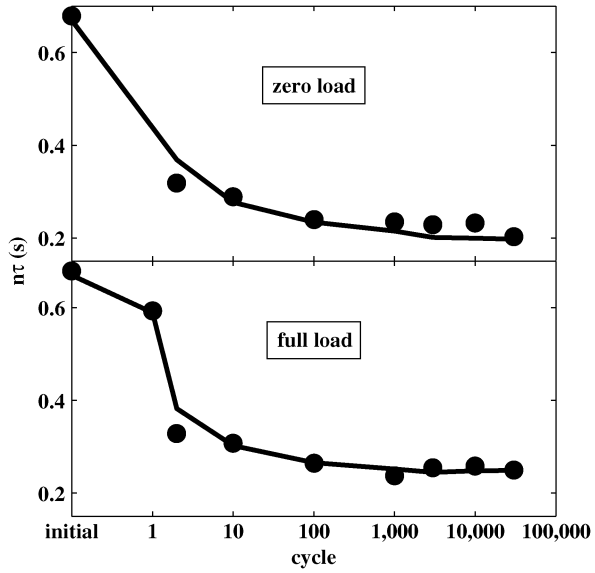

Fig. 5. Symbols represent the coupling loss time constant at zero load (top) and at full load (bottom) with cycles. Lines are fits by intra-petal R_c.

despite its low void fraction, shows an increase by a factor ∼2 and the high void fraction CS1 shows an increase by a factor ∼5. A possible explanation is that with a longer twist pitch, the triplet is less tightly bound.

Another factor to determine the triplet R_c is the number of crossing points between strands. The longer twist pitch in EUTF3 could result in the less number of crossing contacts, that is, a high R_c. From these factors, we interpret that the degree of freedom in the triplet limited by the void fraction determines the distribution of R_c in the prototypes of similar twist pitches, while EUTF3 has a high triplet R_c owing to the greater freedom in the triplet and the less number of crossing points from the longer twist pitch.

IV. Cable Stiffness and Contact Area

The initial displacement of EUTF3 at the maximum load is ∼0.95 mm. With cycles the maximum displacement increases up to ∼1.35 mm at the final cycle. The increase in displacement is similar to the prototypes, however, the initial displacement is greater than CS1 and almost twice greater than the TFMCs (Fig. 4).

As a measure of the stiffness of the conductor, the transverse elastic modulus E_y is evaluated by

$$E_y = \frac{DF_y}{A_y d_y} \tag{1}$$

where D is the cable diameter, A_y is the average longitudinal cable cross section, and d_y is the absolute cable deflection defined relative to the initial condition [6]. The E_y evaluated at the maximum load in the final cycle are compared in Fig. 4. For the prototypes, we find a trend that E_y is higher for lower void fraction.

The low stiffness of EUTF3 may be explained by the overall strand contact area in combination with the strand contact angles. It has been observed that the number of strand contacts is mainly determined by the triplet twist pitch [6] and the void fraction [15], while it is related to the overall cable stiffness. The reciprocal of the triplet R_c i.e. proportional to the overall strand contact area, is plotted together with E_y in Fig. 4. The observed correlation suggests a dependence of E_y on the contact area.

V. Coupling Loss Time Constant

The coupling loss time constant is evaluated from the slope of loss-frequency curve in the low frequency part [1]. Initially, EUTF3 has a high $n\tau \sim 680$ ms (Fig. 5). The $n\tau$ decreases mostly within the first 100 cycles and seems to saturate to final values of ∼200 ms at zero load and ∼250 ms at full load. In the prototypes, we have observed similarly a fast decrease in $n\tau$ in the first 100 cycles. The void fraction seemed to determine both the initial and the final values, and the rate of decrease in the R_c with cycles and, consequently, the evolution of $n\tau$ [5].

In the multiple time constant model [1], [4], [9], we may assume each cabling stages, or equivalent representation of current loops with their specific time constant, contributes to the overall $n\tau$. Although the degree of contributions from each cabling stages is not exactly known, an empirical fit [4] has shown that it is possible to scale $n\tau$ for various conductors with similar cabling patterns, by assuming constant contributions from $n\tau$ associated with cable stages.

The long twist pitches of EUTF3 would result in rather different coupling loops compared to the conductors in [4], and therefore, we will not straightforwardly apply the same empirical fit here. The preceding sections showed that the influence of the long twist pitches is clearly observable in the triplet R_c and also in a degree of correlation between the triplet R_c and the overall stiffness of the conductor. For a comparative analysis, we consider an effective time constant from the triplet stage that is proportional to the square of the twist pitch L_p divided by R_c. Because of the long twist pitch, the calculated ratio L_p^2/R_c is expected to have a high initial value for EUTF3. Although the increased inter-petal coupling may also contribute to a high value of measured initial $n\tau$, the spread in initial $n\tau$ amongst

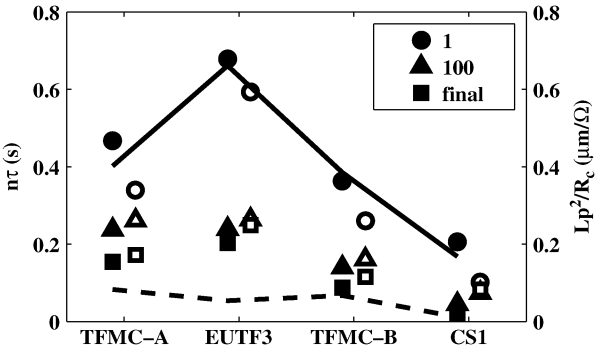

Fig. 6. Symbols for coupling loss time constants at zero load (filled) and at full load (open). Solid line and dashed line are initial and final L_p^2/R_c for triplet at zero load, respectively.

conductors seem to match the spread in the triplet L_p^2/R_c rather well (Fig. 6). For the final $n\tau$ at zero load, we find a good agreement between the increase in the triplet R_c and the decrease in $n\tau$ for the prototypes. For EUTF3, despite the large increase in the triplet R_c, $n\tau$ saturates at $\sim$30% of the initial value.

The same comparative analysis is performed for the intra-petal higher cabling stages. Note that the intra-petal stages are without discontinuities such as wraps. For the prototypes, R_c from the higher intra-petal stages were measured from bundles of strands within a petal. The overall trend is a duplicate of the triplet case shown in Fig. 6 albeit a different magnitude of the calculated L_p^2/R_c. For EUTF3, R_c from the higher intra-petal stages were measured between a pair of strands so no direct comparison can be made against the prototypes. The ratio of contributions from various cabling stages to the overall $n\tau$ such as a fit in [4] is beyond the purpose of a comparative analysis here, since it is not expected to be the same for conductors with very different cabling schemes.

In the case of EUTF3, for the zero load R_c with cycles, all intra-petal stage R_c are increasing and inter-petal R_c is saturating at $\sim$40 times the initial values (Fig. 1). Therefore, the origin of $n\tau$ being saturated at a high value is not obvious from the intra-petal R_c alone. The evolution of $n\tau$ with cycles can be followed by the change in intra-petal R_c, if a constant offset is allowed. With an offset and a multiplicative factor, any one of the intra-petal R_c can fit equally well the evolution of $n\tau$, for instance from the triplet R_c as shown by lines in Fig. 5. In reality, however, the coupling loops are formed by all strands of all cabling stages linked together in a complex pattern. A full numerical model of the coupling loss [7], taking into account the individual strand trajectories, will be used to validate the measurement result.

VI. Summary

A summary of the recent press measurement result of EUTF3 has been presented here using the triplet R_c as a guide for comparison against prototype conductors. We find a high initial triplet R_c, despite the low void fraction, due to the long twist pitch that bounds the triplet less tightly. Consequently, the cable is less stiff than the prototypes with similar void fractions but shorter pitches. A correlation between the stiffness of the conductor and the triplet R_c points to the role of inter-strand contact area and contact periodicity in defining the cable mechanical and electrical properties. We find a high initial $n\tau$ that is in agreement with the long twist pitches. The analysis of the measured $n\tau$ and its progress with cycles by using the numerical model is in progress.

References

[1] A. Nijhuis, N. W. Noordman, H. J. ten Kate, N. Mitchell, and P. Bruzzone, "Electromagnetic and mechanical characterization of ITER CS-MC conductors affected by transverse cyclic loading, part 1: Coupling current loss," *IEEE Trans. Appl. Supercond.*, vol. 9, pp. 1069–1072, 1999.

[2] A. Nijhuis, N. W. Noordman, H. J. ten Kate, N. Mitchell, and P. Bruzzone, "Electromagnetic and mechanical characterization of ITER CS-MC conductors affected by transverse cyclic loading, part 2: Interstrand contact resistances," *IEEE Trans. Appl. Supercond.*, vol. 9, pp. 754–757, 1999.

[3] A. Nijhuis, N. W. Noordman, O. A. Shevchenko, H. J. ten Kate, and N. Mitchell, "Electromagnetic and mechanical characterization of ITER CS-MC conductors affected by transverse cyclic loading, part 3: Mechanical properties," *IEEE Trans. Appl. Supercond.*, vol. 9, pp. 165–168, 1999.

[4] A. Nijhuis, Y. Ilyin, W. Abbas, B. ten Haken, and H. H. J. ten Kate, "Change of interstrand contact resistance and coupling loss in various prototype ITER NbTi conductors with transverse loading in the Twente Cryogenic Cable Press up to 40,000 cycles," *Cryogenics*, vol. 44, pp. 319–339, 2004.

[5] A. Nijhuis, Y. Ilyin, W. Abbas, H. H. J. ten Kate, M. V. Ricci, and A. della Corte, "Impact of void fraction and evolution of coupling loss in ITER Nb3Sn conductors under cyclic load," *IEEE Trans. Appl. Supercond.*, vol. 15, pp. 1633–1636, 2005.

[6] A. Nijhuis and Y. Ilyin, "Transverse cable stiffness and mechanical losses associated with load cycles in ITER $\mathrm{Nb_3Sn}$ and NbTi CICCs," *Supercond. Sci. Technol.*, vol. 22, p. 055007, 2009.

[7] E. P. A. van Lanen and A. Nijhuis, this conference.

[8] A. Nijhuis, H. H. J. ten Kate, P. Bruzzone, and L. Bottura, "Parametric study on soupling loss in subsize ITER Nb3Sn cabled specimen," *IEEE Trans. Magn.*, vol. 32, pp. 2743–2746, 1996.

[9] T. Schild and D. Ciazynski, "A model for calculating a.c. losses in multistage superconducting cables," *Cryogenics*, vol. 36, pp. 1039–1049, 1996.

[10] K. Seo, K. Fukuhara, and M. Hasegawa, "Analyses for inter-strand coupling loss in multi-strand superconducting cable with distributed contact resistance between strands," *Cryogenics*, vol. 41, pp. 131–137, 2001.

[11] L. Bottura, M. Breschi, and C. Rosso, "Analysis of electrical coupling parameters in superconducting cables," *Cryogenics*, vol. 43, pp. 233–239, 2003.

[12] A. Nijhuis and Y. Ilyin, "Transverse load optimization in $\mathrm{Nb_3Sn}$ CICC design; Influence of cabling, void fraction and strand stiffness," *Supercond. Sci. Technol.*, vol. 19, pp. 945–962, 2006.

[13] P. Bruzzone *et al.*, "Test results of two European ITER TF conductor samples in SULTAN," *IEEE Trans. Appl. Supercond.*, vol. 18, pp. 1088–1091, 2008.

[14] J. Lu, V. Toplosky, K. Han, T. Adkins, S. T. Bole, and R. P. Walsh, "The inter-strand contact resistance of $\mathrm{Nb_3Sn}$ cable-in-conduit conductor with hydrocarbon oil," *Supercond. Sci. Technol.*, vol. 21, p. 115011, 2008.

[15] N. Mitchell, "Operating strain effects in $\mathrm{Nb_3Sn}$ cable-in-conduit conductors," *Supercond. Sci. Technol.*, vol. 18, pp. S396–S404, 2005.